ACI STRUCTURAL JOURNAL TECHNICAL PAPER

Title No. 113-S107

Size Effect in Torsional Strength of Plain and Reinforced Concrete

by Kedar Kirane, Konjengbam Darunkumar Singh, and Zdeněk P. Bažant

As shown long ago, plain and longitudinally reinforced concrete beams without stirrups exhibit a significant size effect on torsional strength, which was thought to be of a type occurring after long, stable crack growth (called Type II). This paper shows, by experimentally calibrated finite element simulations, that: 1) longitudinally reinforced concrete beams with stirrups also exhibit a significant size effect; and 2) the size effect in beams both with and without stirrups is not of Type II but Type I, characterizing failure at macrocrack initiation. In the practical size range, Type I is deterministic and terminates with a horizontal, rather than inclined, asymptote. The simulations are based on microplane model M7, which was shown to match well all the types of uniaxial, biaxial, and triaxial tests with post-peak softening in tension and compression. The model is calibrated by simulating previous torsional size effect tests of plain concrete beams and of longitudinally reinforced beams without stirrups, as well as the tests of beams with stirrups having different reinforcement ratios and different aspect ratios. The fact that all these tests are fitted closely, in terms of not only the maximum loads but also the crack patterns, lends credence to the predictions of size effect in beams with stirrups.

Keywords: crack band model; microplane model; reinforced concrete; size effect; torsion.

INTRODUCTION

In the past few decades, significant research effort has been dedicated to studying the torsional behavior of concrete structural members. There have been several studies devoted to developing analytical models to predict the elastic stress distribution and strength limits of concrete beams under torsion (refer to Reference 1 for a comprehensive review). Important advances have been made in many experimental studies aimed at understanding the effect of various physical and geometrical parameters on the torsional strength of concrete beams, such as the aspect ratio, reinforcement ratio, and compressive strength.[1-13] However, the size effect on torsional strength has been studied only for beams without stirrups, which are not used in practice when torsion dominates. These previous studies, which included rectangular plain concrete beams and reinforced concrete beams without stirrups made with reduced-size aggregate,[4,5,14] documented the existence of a strong size effect but did not include finite element simulations and did not reveal whether the size effect is Type II, such as in shear of beams and punching of slabs, or Type I.

The Type I size effect occurs if the failure occurs at crack initiation from a smooth surface or an edge. It has, in the log-strength versus log-size plot, a convex curvature. For large sizes, it transits to the Weibull statistical size effect, but concrete beam sizes are generally not large enough for statistics to intervene. The Type I deterministic size effect has a lower bound. The Type II size effect is always deterministic and occurs when a large crack grows stably prior to the maximum load. It has a concave curvature, no lower bound, and terminates with an asymptotic straight line of slope −1/2. To ensure safe and reliable torsion designs of real-world structures based on a physically sound extension of laboratory-scale data, it is crucial to understand the size effect type, especially for beams with stirrups.

The purpose of this study is to use a state-of-the-art damage constitutive model to develop and validate a finite element model for the torsional size effect, use this model to determine the size effect type, and validate a simple size effect law for torsion. The model will be calibrated by the available experimental data on torsional failures of plain concrete beams and longitudinally reinforced concrete beams with and without stirrups (all of them unnotched). Although beams without stirrups and plain concrete beams cannot be used in practice for torsional loading, their tests are useful for model calibration. Only unnotched beams of solid rectangular cross sections will be considered. The torsion of box girders is not covered, but their analysis with the microplane model will be more credible if that model is validated at least for solid rectangular cross sections in torsion.

RESEARCH SIGNIFICANCE

Without an understanding of the size effect and its type, the laboratory-scale torsional strength tests cannot be reliably extrapolated to the large beams used in practice. The present study takes a step toward overcoming this gap of knowledge. While the previous torsional size effect studies dealt only with beams without stirrups, the present study includes stirrups as well. Although scaled torsional strength tests of reinforced box cross sections, which are the typical choice in design of large girders, are unavailable, the fact that the present general mathematical model is successfully validated by tests of size effect in solid rectangular cross sections with and without stirrups will lend credence to the use of this model in box girder design. Furthermore, the present determination of the size effect type will make extrapolations to large beams more reliable.

NUMERICAL APPROACH

The microplane model M7[15] is the latest version in a series of progressively improved microplane models labeled M0,

ACI Structural Journal, V. 113, No. 6, November-December 2016.

MS No. S-2015-250.R2, doi: 10.14359/51689149, received November 22, 2015, and reviewed under Institute publication policies.

M1, M2...M6, developed primarily for concrete.[16,17] Supplemented by a localization limiter with material characteristic length, it has been proven to give rather realistic predictions of the constitutive, damage, and fracture behavior of quasi-brittle materials over a broad range of loading scenarios, including uniaxial, biaxial, and triaxial loadings with post-peak softening, compression-tension load cycles, opening and mixed mode fractures, tension-shear failure, and axial compression followed by torsion.[18]

The basic idea of the microplane model is to express the constitutive law not in terms of tensors, but in terms of the vectors of stress and strain acting on a generic plane of any orientation in the material microstructure, called the "microplane." Considering all such planes capture the interactions among various orientations, which makes the model semi-multi-scale in nature (a fully multi-scale model must also capture interactions at distance). The use of vectors was inspired by an idea of Taylor[19] and is also a characteristic of Taylor models for hardening plasticity of polycrystalline metals.[20] However, there are important conceptual differences. First, to avoid model instability due to post-peak softening in concrete, a static constraint of the microplanes is replaced by a kinematic one.[17] Thus, the strain (rather than stress) vector on each microplane is the projection of the macroscopic strain (rather than stress) tensor. Second, a variational principle (principle of virtual work) is introduced to relate the stresses on the microplanes of all possible orientations to the macro-continuum stress tensor so as to ensure equilibrium. Formulated in terms of stress and strain vectors rather than vectors, the constitutive law can simulate cracks and frictional slips of specific orientations. Dilatancy due to shear and vertex effect are automatically captured by interaction of microplanes of different orientations. The microplane model M7 was incorporated into the commercial finite element code ABAQUS, version 6.11, using the material subroutine VUMAT.[21]

A typical problem in finite element extrapolation of limited test data is that different combinations of material parameters can often fit the same data. This is particularly true for primitive triaxial constitutive laws. There are at least 100 of them in the literature, but each of them can fit only a few among the 22 different types of triaxial tests successfully fitted by the microplane model, which is the reason why the extrapolation of test data is often ambiguous. For the microplane model, the ambiguity is low. One parameter—the radial scaling parameter k_1—sufficed to get a good fit of the peak loads, and mild adjustment of parameters k_2 and k_3 sufficed to adjust the fit of post-peak softening in the torsional test data. The remaining parameters were kept fixed as calibrated a priori for all concretes in the microplane model development.[15,18] Of course, one might conceivably be able to fit the torsional data with other values of the remaining parameters, but then the fit of the 22 types of triaxial tests used in previous general calibration of microplane model would be lost.

To prevent spurious mesh sensitivity, particularly the dependence of failure loads on the chosen mesh size, the modeling was performed in the sense of the crack band model,[22] where the band width h is a material property acting as the localization limiter. The band width is the minimum possible spacing of parallel macrocracks, and previous studies showed that for normal concretes it may be taken as approximately double the maximum aggregate size.[8,22] If, for computational reasons, an element size different from h needs to used, the post-peak softening of the material model must be rescaled to preserve the same fracture energy. However, the crack band model is most accurate if the mesh size is kept the same, which is what was done here.

A variety of concrete beams previously tested were modeled. The beams of all sizes under consideration were meshed by four-node tetrahedral elements (C3D4) of average size h. The mesh was regular but randomized and, thus, almost free of directional bias in the global sense. This randomness is important for predicting the correct overall crack direction and path when the crack band model is used. With the proper mesh size, herein taken as the double of the maximum aggregate size, the free parameters of the microplane model M7 were calibrated to match the test data (such as torsional strength and torque-twist curves). After calibration, the size effect in the nominal torsional strength v_u of the beams was analyzed. To speed up the explicit dynamic integration, the natural time scale, irrelevant to statics, was contracted by mass scaling[21] (that is, artificial scaling of material density). The scaling factor of 100 was chosen. The nominal torsional strength v_u for beams of rectangular cross section was defined as[1,4]

$$v_u = \frac{T_{max}}{\alpha B^2 D}, \text{ where } \alpha = \frac{1}{2}\left(1 - \frac{B}{3D}\right) \tag{1}$$

where T_{max} is peak torque; and B and D are shorter and longer sides of the rectangle. Although this is a plastic limit analysis formula, coefficient α was based on the elasticity solution, as usual.[1]

NUMERICAL RESULTS AND DISCUSSION: TEST DATA SET I[5]

First, consider the torsion tests of plain and longitudinally reinforced concrete beams with strict geometric scaling[5] (that is, scaling in which all the structure dimensions are scaled in the same ratio). The beams had a square cross section with side D and length $L = (8/3)D$. Beams of three sizes (small, medium, and large), D = 38.1, 76.2, and 152.4 mm [1.5, 3, and 6 in.], were tested. The reinforcement ratios were also scaled accordingly. A reduced maximum aggregate size of 4.8 mm (0.189 in.) was used, to limit beam sizes (for details, refer to Reference 5). The crack band for the simulations by M7 was set as 7.5 mm (0.295 in.), which was roughly 1.5 times the maximum aggregate size. The M7 parameters were calibrated using data for plain concrete, whereas the validation used data on longitudinally reinforced concrete beams without stirrups.

Although according to current design codes, the beams subjected to significant torque are required to have stirrups, first analyzed will be the beams without stirrups, which is helpful for a complete understanding.

Plain concrete beams

The measured and predicted nominal strengths for plain concrete beams are compared in Fig. 1 and the adjusted parameters are listed in Table 1. The plots of predicted torque T (normalized with respect to T_{max}) versus twist and the shear stress v (= $T/\alpha B^2 D$) versus twist are shown in Fig. 2(a) and 2(b). It is seen that, for each size, the failure occurs as soon as the peak torque is reached and no stable crack growth occurs before the peak. The torque drop after the peak is vertical and dynamic, indicating snap-back on the equilibrium path (this means that the post-peak descending load-displacement curve reverts from negative to positive slope, which is unstable under both load and displacement control).

The salient feature of the crack band model is its capability to predict the localization pattern in structures. This is verified by the plots of the maximum principal strain at peak torque shown for each size in Fig. 3. Indeed, these plots faithfully reproduce the experimentally observed failure patterns.[5] In particular, the predicted crack surface has the mean inclination of 45 degrees, and is slightly warped on one side, terminating with a smaller inclination at the opposite side.

Consider now the predicted size effect on torsional strength, shown in Fig. 1. Similar to experiments, it is strong. Determining the size effect type from the tests is hard because of scatter and limited size range, and also because it is not easy to ascertain whether the dynamic post-peak propagation started at zero or finite crack length. This uncertainty can be overcome by modeling, in which a broad enough size range is considered and the scatter is far smaller because its source is mainly the randomness of the mesh, such as the mesh direction bias and small random variations of mesh size, which have more effect for smaller sizes as the mesh is coarser relative to beam size.

The torsional failure, as observed herein, is brittle, occurring right at crack initiation from a smooth surface. Consequently, the energy release from the structure vanishes and the size effect is due solely to stress redistribution caused by a large fracture process zone. This typically implies the existence of a Type I size effect,[23] characterized by a positive curvature of the log-log plot of nominal strength versus characteristic size, as seen in Fig. 1. The large-size asymptote of Type I size effect is a horizontal line if only the energetic (or stress redistribution) aspect is considered.

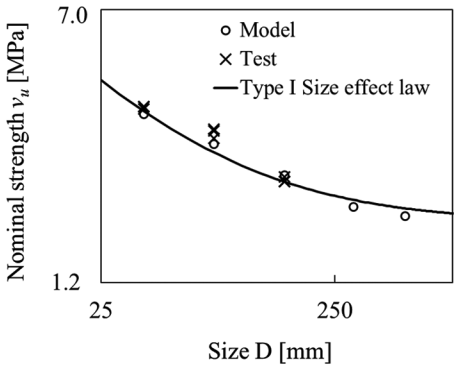

Fig. 1—Comparison of predicted and measured[5] nominal torsional strengths for plain concrete beams. (Note: 1 mm = 0.0394 in.; 1 MPa = 0.145 ksi.)

Table 1—Elastic material constants and parameters of microplane model M7

Material parameter unit (secondary unit)	Data Set I[5]	Data Set II[2,3]
Young's modulus of concrete, E, MPa (ksi)	26,000 (3770.9)	35,000 (5076.32)
Poisson's ratio	0.18	0.18
Compressive strength f_c' (28 days), MPa (ksi)	43.87 (6.36)	28.6 (4.14)
Density of concrete, kg/m^3 (lb/in.^{3})	2800 (0.1011)	2400 (0.0867)
Radial scaling parameter k_1	95×10^{-6}	50×10^{-6}
k_2	110	110
k_3	30	15
k_4	100	60
k_5	1	1
k_6	1×10^{-4}	1×10^{-4}
k_7	1.8	1.8
Young's modulus of steel, GPa (ksi)	200 (29,007.54)	185 (26,831.97)
Poisson's ratio	0.3	0.3
Yield strength, MPa (ksi)	413 (59.9)	325 (47.14)
Density of steel, kg/m^3 (lb/in.^{3})	7850 (0.2836)	7850 (0.2836)

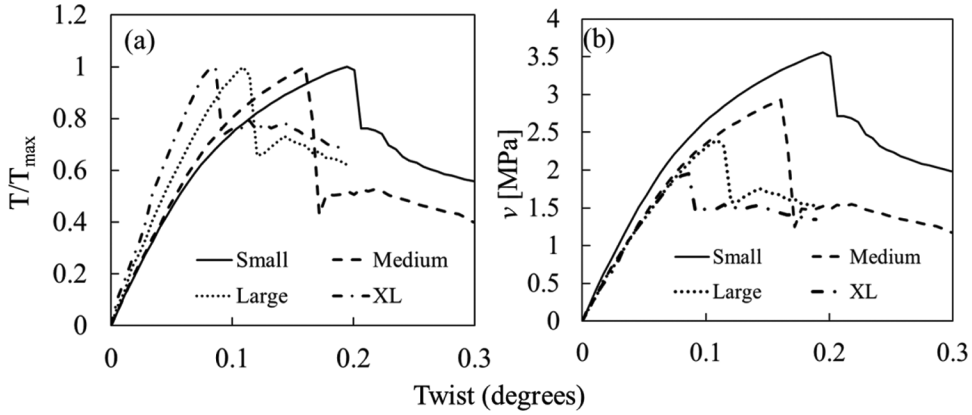

Fig. 2—Predicted (a) torque-twist curves; and (b) shear stress-twist curves, for plain concrete beams of different sizes; same beams as in Bažant et al.[5] tests. (Note: 1 MPa = 0.145 ksi.)

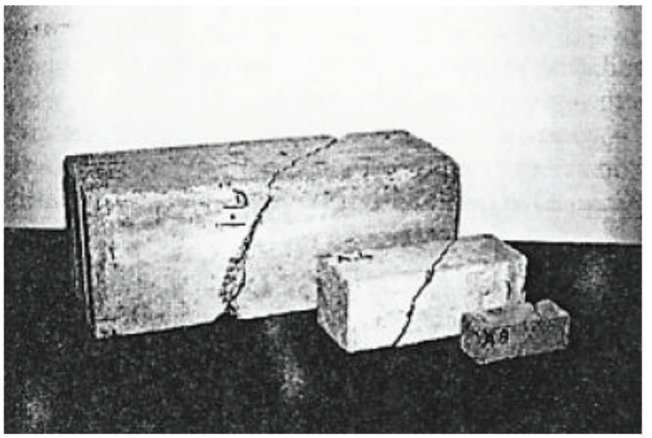

(a)

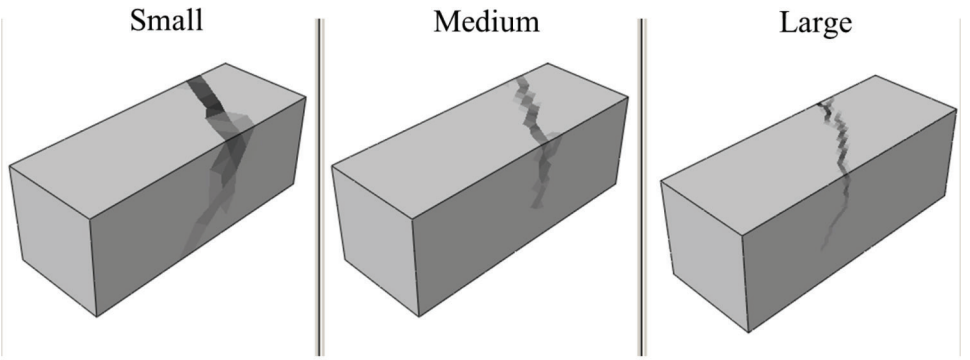

(b)

Fig. 3—(a) Observed[5]; and (b) predicted failure patterns for plain concrete beams of different sizes.

By contrast, the Type II size effect occurs in failures such as shear failure of beams or punching failure of slabs, in which either a large crack grows in a stable manner prior to reaching the maximum load or a large notch exists. This is a fundamental difference from the torsional failures, even though both can be regarded as shear failures. Mathematically, the Type II size effect is determined by the energy release rate from the structure.

For very large beams, the Type I size effect results from a combination of stress redistribution with the Weibull statistical size effect, the latter being explained by the weakest-link model. The present beams, however, are not large enough, and so the present deterministic modeling is sufficient, although in general the method to combine the deterministic size effect with the statistical one for large sizes is well known. It suffices to replace the horizontal asymptote with a tangent inclined asymptote of slope $-n/m$, where m is the Weibull modulus and n is the number of failure dimensions ($m = 24$ for concrete).[24] The physical reason why the Type II size effect does not occur for torsion is that no large stable crack can grow before the peak load, and the failure under controlled load occurs right at the peak load.

To verify the approach to an asymptote, characterizing the Type I size effect, a supercomputer was used to also simulate plain concrete beams of much larger sizes than those tested, namely, $D = 300$ mm (11.81 in.) (XL) and 500 mm (19.68 in.) (XXL); refer to the nominal torsional strengths plotted in Fig. 1, which demonstrate that the large-size asymptote tends to a horizontal line and thus confirms that the size effect is of Type I. The deterministic Type I size effect reads

$$v_u = v_{u\infty}\left(1+\frac{rD_b}{D}\right)^{1/r} \tag{2}$$

where $v_{u\infty}$ is the torsional strength corresponding to an infinitely large specimen ($D \to \infty$); r and D_b are material parameters; and D_b represents a transitional size constant proportional to the thickness of the boundary layer of cracking. Previous optimal fitting of the test data[23] provided $r = 1.47$. Due to lack of data for torsion, $r = 1.5$ is assumed herein. Then, the optimal fitting of Eq. (2), indicated by the solid curve in Fig. 1, yields $v_{u\infty} = 1.77$ MPa (256.65 psi) and $D_b = 49.3$ mm (1.94 in.).

This behavior contrasts with the Type II size effect, which applies to geometries where a large stress-free crack (or a notch) exists at peak load. Then, the size effect on mean strength is purely deterministic, the curvature is negative, and the large-size asymptote has a slope of –1/2, which corresponds to the scaling predicted by linear elastic fracture mechanics (LEFM). In previous work,[1,4,5] for lack of data of sufficient size range, a Type II size effect was assumed to exist in the torsional strength. The present study rectifies this unjustified assumption.

Longitudinally reinforced concrete beams without stirrups

Based on the calibrated model, predictions are now made for longitudinally reinforced concrete beams without stirrups. Beams of rectangular cross sections and the same sizes as for plain concrete were tested. The reinforcement consisted of four longitudinal bars placed in the cross section corners, with the cover of 8.1, 16.3 and 31.5 mm (0.319, 0.642, and 1.24 in.), proportionally scaled for the small, medium, and large sizes. The respective diameters of the bars were 3.18, 6.35, and 12.7 mm (0.125, 0.25, and 0.5 in.). The corresponding longitudinal reinforcement ratio ρ_l was 1.9% for each size. The material properties used for steel are listed in Table 1. The reinforcement was modeled by two-node truss elements (T3D2) embedded in the solid host elements of concrete, with no slip at nodes. The size of the truss elements was also maintained equal to h.

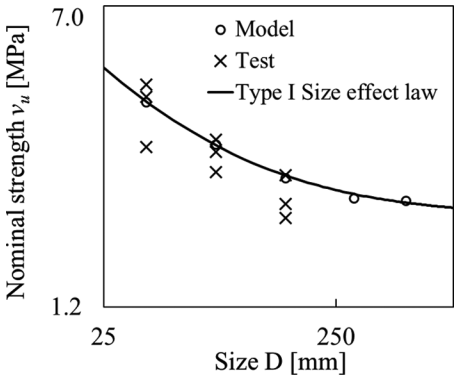

Fig. 4—Comparison of predicted and measured[5] nominal torsional strengths for longitudinally reinforced concrete beams. (Note: 1 mm = 0.0394 in.; 1 MPa = 0.145 ksi.)

Figure 4 shows the comparison of the measured and predicted nominal torsional strengths, calculated according to Eq. (1). Despite the large scatter in test data, the agreement can be considered satisfactory and serves as validation of the predictions. The simulations showed that, even for longitudinally reinforced beams, the peak load occurs when the crack initiates from the beam edge and no stable crack growth prior to the maximum load (which is different from the shear failure of reinforced beams). However, the torque herein does not drop suddenly after the peak load. Rather, it decreases gradually in a series of small increases and small but bigger vertical drops (refer to Fig. 5(a) and 5(b)). In fact, for larger sizes, the post-peak response is almost perfectly plastic, with a horizontal plateau. This difference in behavior is obviously caused by the longitudinal reinforcement. However, in spite of this difference, the torsional capacity of the beams is not affected much. Figure 6 shows the predicted failure pattern at peak, which looks very similar to that in plain concrete beams. This suggests that the type of size effect should not change. This is confirmed by the positive curvature of the size effect plot in Fig. 4. For verification of the large-size asymptote, simulations were also run for two additional sizes. They were (as before) D = 300 and 500 mm (11.81 and 19.68 in.), with correspondingly scaled dimension, including the covers and diameters of reinforcement, thus maintaining strict geometric similarity. The nominal strengths for these sizes are also shown in Fig. 4, which indi-

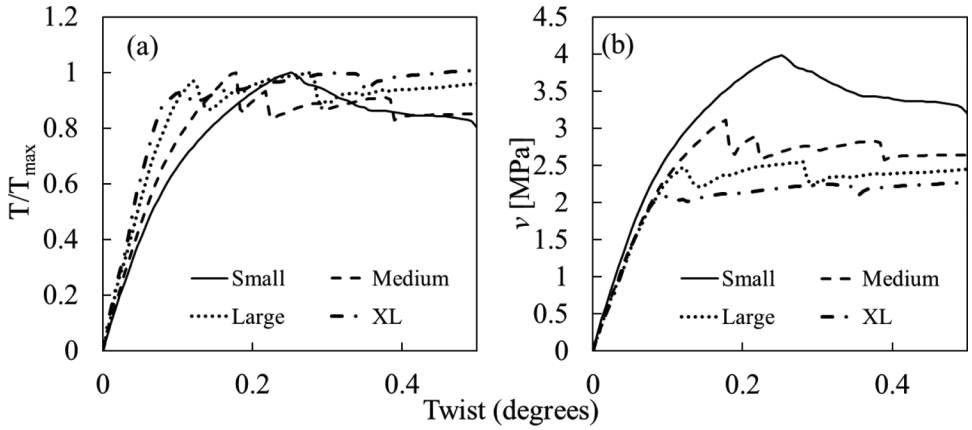

Fig. 5—Predicted (a) torque-twist curves; and (b) shear stress-twist curves, for longitudinally reinforced beams of different sizes; the same beams as in Bažant et al.[5] tests. (Note: 1 MPa = 0.145 ksi.)

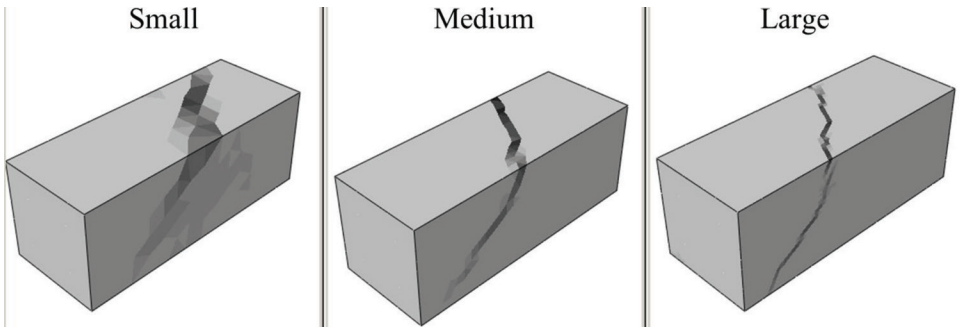

Fig. 6—Predicted failure patterns for longitudinally reinforced beams of different sizes, tested by Bažant et al.[5]

cate that the large-size asymptote tends to a horizontal line. This confirms that the size effect is of Type I. Assuming r = 1.5 (which yields the best fit in this case), $v_{u\infty}$ = 2.03 MPa (294.35 psi), and D_b = 44.2 mm (1.74 in.), the values are not too different from those for plain concrete.

Longitudinally reinforced concrete beams with stirrups

As confirmed in the preceding section, the longitudinal reinforcement does not increase the torsional capacity, although it does make the failure less brittle. A significant capacity and ductility increase is attained by introducing stirrups, which is why they are required by current codes. Unfortunately, no tests of size effect with strict geometric scaling exist for stirrups, so the size effect is analyzed purely numerically. The calibration of the model for beams without stirrups is what lends credibility to the analysis.

Each beam contains 10 stirrups, evenly spaced, in addition to the longitudinal reinforcement (Fig. 7). The total reinforcement ratio was kept fixed at 4.19% for all sizes (the stirrup ratio was ρ_t = 1% and longitudinal ρ_l = 2.19%). Like the longitudinal bars, the stirrups were also meshed with two-node truss elements of length h. Torsion simulations were conducted in the same way as before. Beams of only four, instead of five, sizes were simulated.

Figures 8(a) and 8(b) show the computed torque-twist curves and stress-twist curves, which reveal further differences in behavior. The torque (and stress) initially rises until the strain localizes into a narrow band, which can be regarded as cohesive crack. Subsequently, though, the torque does not decrease. Rather, it continues to rise with a smaller slope. The torque eventually reaches a peak and then begins to drop gradually. Thus, there is a pronounced cohesive crack growth that occurs before the peak condition is reached. These results illustrate the effectiveness of stirrups in preventing sudden torsional failures and increasing the torsional capacity of the beams. Figure 9 shows the failure pattern in the first three sizes in a later stage of post-peak softening. The failure geometry of the dominant crack is similar to the previous two cases, but there are more inclined cracks. Further, the torque-twist response is very different.

The calculated nominal torsional strength is plotted against the size in the log-log plot of Fig. 10. The curvature is again positive, which is indicative of a Type I size effect. This is a curious result because, typically, when a crack initiates and

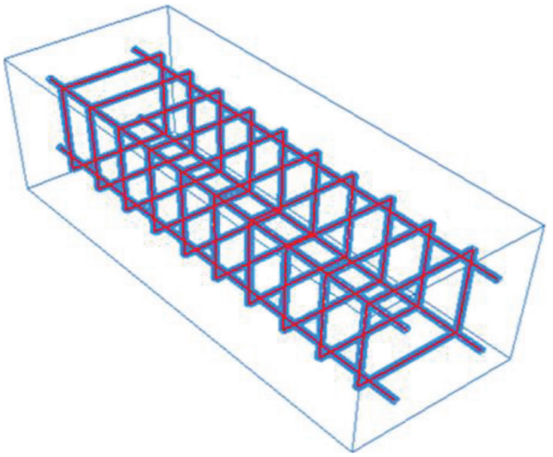

Fig. 7—Stirrup geometry.

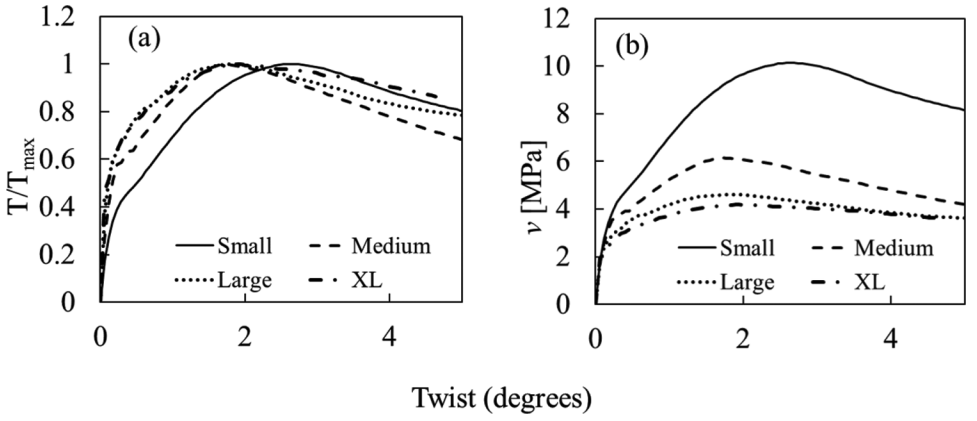

Fig. 8—Predicted: (a) torque-twist curves; and (b) shear stress-twist curves, for concrete beams, with stirrups (reinforcement ratio = 4.19%). (Note: 1 MPa = 0.145 ksi.)

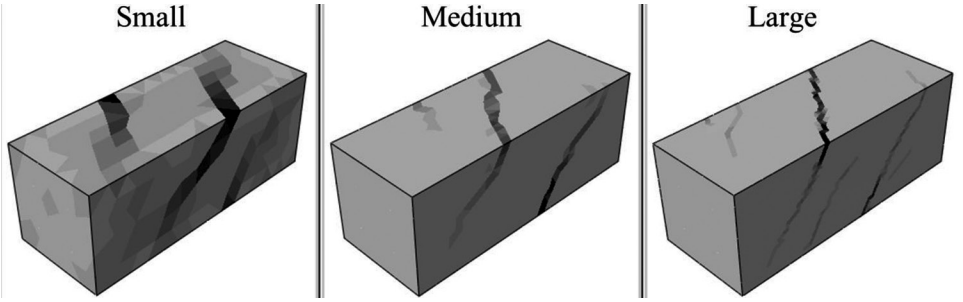

Fig. 9—Predicted failure patterns for concrete beams, with stirrups (reinforcement ratio = 4.19%).

stably grows before the overall peak load is reached, a Type II size effect is manifested.[14] This is not the case here, probably because, despite localization, a stress-free crack does not exist at peak load and the PFZ has not yet moved away from the corner. This was revealed by querying the stresses in the elements lying on the surface with the highest strain levels, within the crack band. So, it is concluded that the size effect is of Type I, the same as without stirrups. Equation (2) for Type I size effect is fitted in Fig. 10 to the calculated points, which yields $v_{u\infty}$ = 3.24 MPa (469.8 psi) and D_b = 80.4 mm (3.165 in.), for r = 1.5. Note that now $v_{u\infty}$ is much higher, indicating the increased torsional capacity due to stirrups.

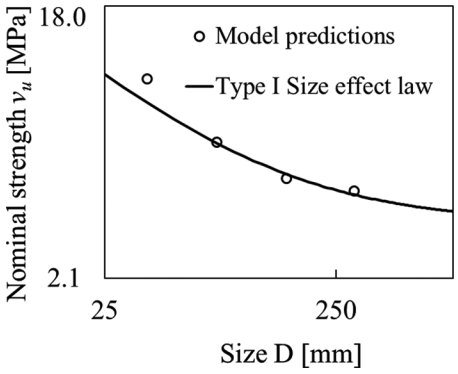

Fig. 10—Predicted size effect in concrete beams with stirrups (reinforcement ratio = 4.19%). (Note: 1 mm = 0.0394 in.; 1 MPa = 0.145 ksi.)

Effect of reinforcement ratio

The size effect was also analyzed for different reinforcement ratios, equal to 1.05% and 8.82%; refer to the torque-twist plots in Fig. 11. For the lower reinforcement ratio, the load actually drops after the crack initiates, but continues to rise subsequently. Apart from this difference, the overall behavior is similar for all three reinforcement ratios. The size effect plots for these two cases are shown in Fig. 12. In each case, a Type I size effect is evident and the same explanation as before applies here as well. The optimal values are $v_{u\infty}$ = 2.16 MPa (313.2 psi), D_b = 39.3 mm (1.55 in.) for ratio 1.05%, and change to $v_{u\infty}$ = 3.39 MPa (491.55 psi), D_b = 95.6 mm (3.76 in.) for ratio 8.82%. These changes are consistent with the finding that stirrups make the failure more ductile.

RESULTS AND DISCUSSION: TEST DATA SET II

Torsion tests of plain and longitudinally reinforced concrete beams without strict geometric scaling[2,3] were analyzed next. In these tests, the effect of parameters other than size, such as the aspect ratio and the reinforcement ratio, was studied systematically. Fitting these data serves to calibrate the model, and success in fitting also provides validation. The calibrated and validated model is then used to analyze the size effect numerically.

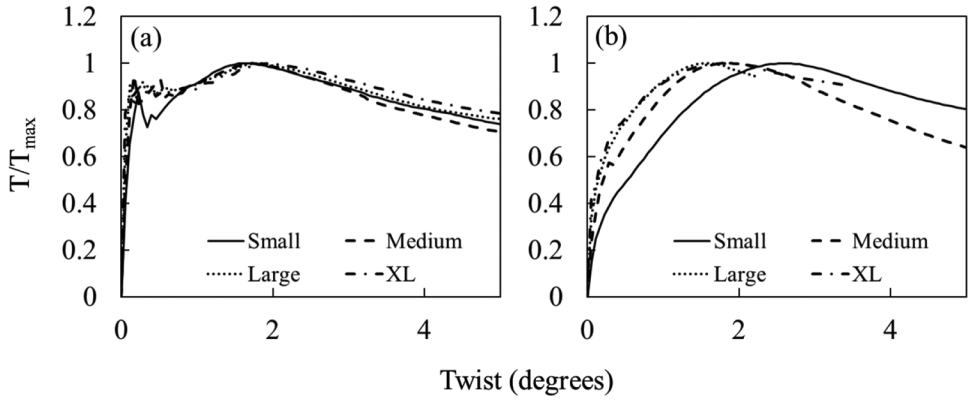

Fig. 11—Predicted torque-twist curves for concrete beams with stirrups: (a) reinforcement ratio = 1.05%; and (b) reinforcement ratio = 8.82%.

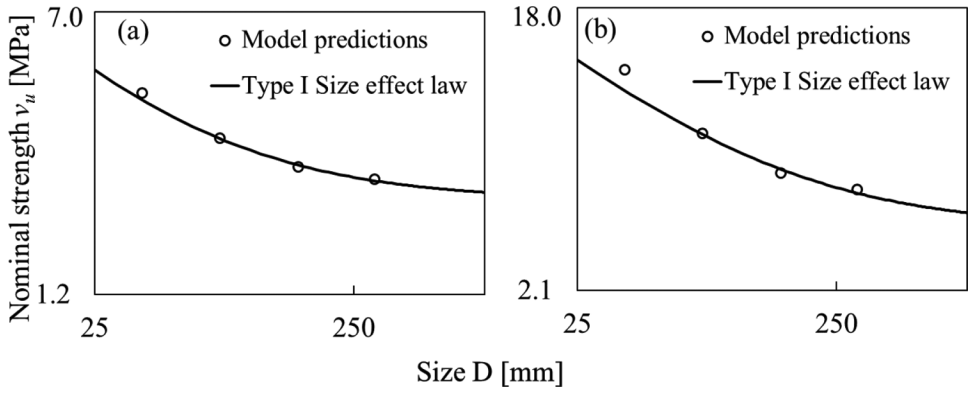

Fig. 12—Predicted size effect for concrete beams with stirrups: (a) reinforcement ratio = 1.05%; and (b) reinforcement ratio = 8.82%. (Note: 1 mm = 0.0394 in.; 1 MPa = 0.145 ksi.)

Effect of aspect ratio

The beams in this data set were plain concrete with maximum aggregate size of 19.5 mm (0.768 in.) and rectangular cross sections.[2] Beams of five different aspect ratios were tested, with two specimens per ratio; refer to Table 2 (the same beam labels are preserved herein). The crack band width h in computations was 40 mm (1.574 in.), which is roughly twice the maximum aggregate size. Finite element models for the plain and reinforced concrete beams were built and meshed with four-noded tetrahedral elements of average size h. The scaling parameters of microplane model M7 were calibrated to match the torque twist-response of Beams A1 and A2; refer to Table 1. The combined size and shape effect in the other beams was predicted using the calibrated model. Consistent with the earlier results, the failure is brittle (sudden load drop), occurring as soon as the crack initiates. A comparison of the experimental and predicted torque twist curves is shown in Fig. 13(a) and that of the maximum torque in Fig. 13(b). The results are seen to be in good agreement with the data, which provides an additional validation of the model.

Table 2—Summary of beams from test data set II[2,3]

Beam ID	Aspect ratio, mm x mm (in. x in.)	Beam ID	Reinforcement ratio, %
A1, A2	254 x 381 (10 x 15)	B1	1.07
A3, A4	254 x 254 (10 x 10)	B2	1.65
A5, A6	254 x 508 (10 x 20)	B3	2.34
A7, A8	152.4 x 279.4 (6 x 11)	B4	3.21
A9, A10	152.4 x 495.3 (6 x 19.5)	B5	4.24
		B6	5.28

Effect of reinforcement ratio

Tests of rectangular concrete beams of cross section 254 x 381 mm (10 x 15 in.), with six different reinforcement ratios, were reported.[3] The reinforcement consisted of longitudinal bars as well as stirrups. The total reinforcement ratio for the various beams (B1 to B6) is shown in Table 2. The geometry of the stirrups can be found in Reference 3 and is not described here for brevity. Using the calibrated model, the response of these beams was predicted. No parameters of the microplane model were changed. The material properties of the reinforcement are shown in Table 1. Figure 14(a) shows a comparison of the predicted torque twist curves with the test data, while Fig. 14(b) shows that for the maximum torque. Again, the agreement is very good, establishing further the predictive capabilities of the model.

Size effect

Next, the calibrated model was used to predict the size effect on torsional strength, considering Beam B3, of characteristic size D, as the basis and scaling it geometrically to other sizes. Five different sizes were considered: 0.5D, D, 2D, 4D, and 6D. Thus, a size range of 1:12 was simulated. Three

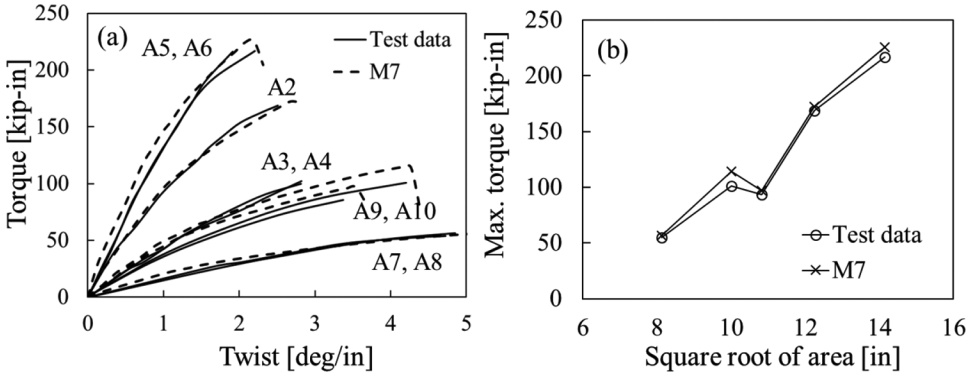

Fig. 13—Comparison of measured[2] and predicted: (a) torque-twist curves; and (b) maximum torque, for plain concrete beams of various aspect ratios. (Note: 1 mm = 0.0394 in.; 1 kip-in. = 112.98 N-mm.)

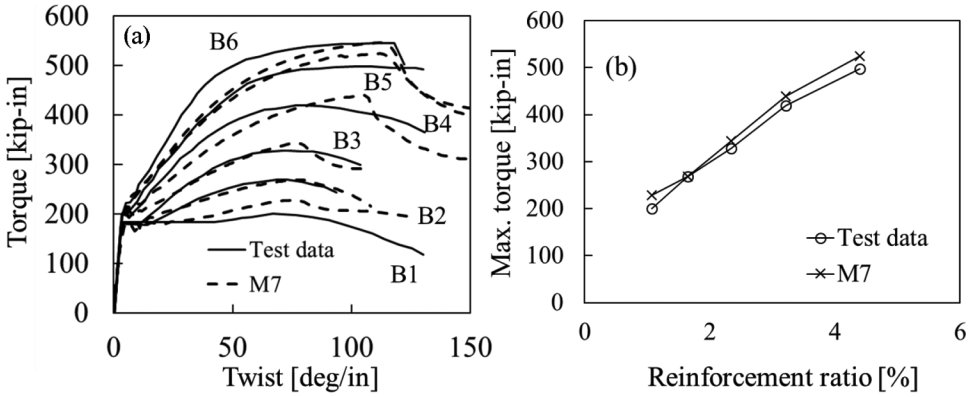

Fig. 14—Comparison of meaured[3] and predicted: (a) torque-twist curves; and (b) maximum torque, for reinforced concrete beams with various reinforcement ratios. (Note: 1 kip-in. = 112.98 N-mm.)

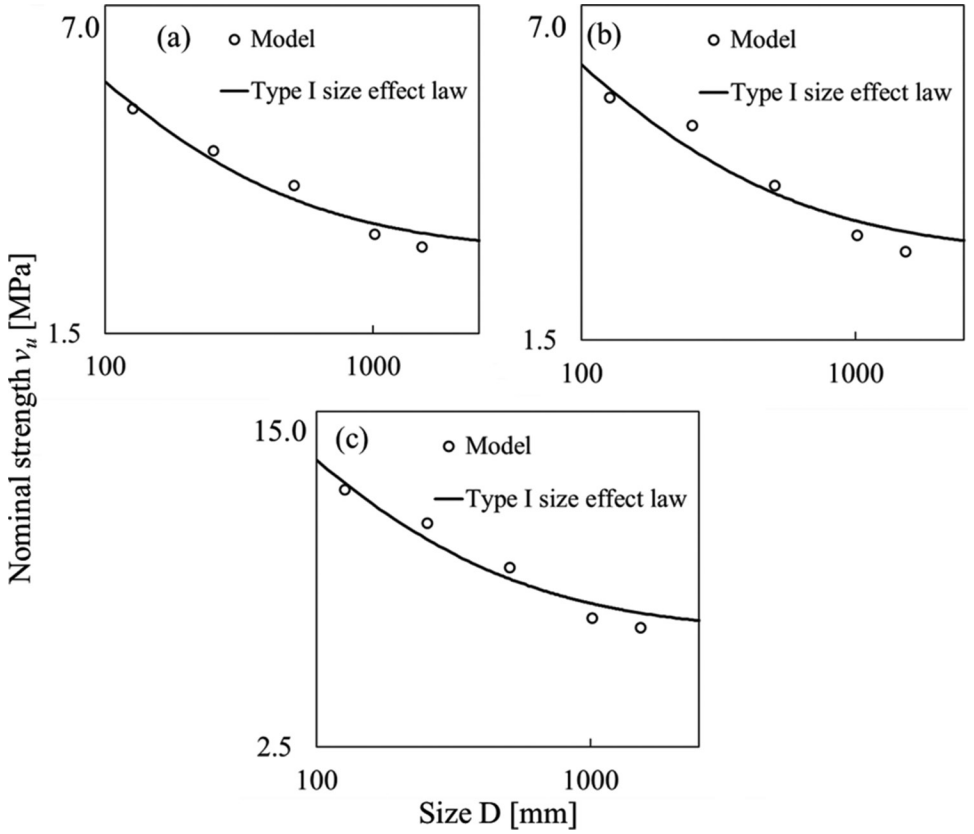

Fig. 15—Predicted size effect for: (a) plain concrete beams; (b) longitudinally reinforced beams without stirrups; and (c) longitudinally reinforced beams with stirrups. (Note: 1 mm = 0.0394 in.; 1 MPa = 0.145 ksi.)

cases were analyzed, like before: 1) plain concrete beams; 2) longitudinally reinforced beams without stirrups; and 3) ditto, but with stirrups. Thus, in all, the torsional response of 15 different beams was simulated. The peak torque was obtained for each case and plotted against the size, as seen in Fig. 15(a), 15(b), and 15(c). It is seen that, for each case, the curvature of log-log plot indicates a size effect of Type I. The solid curve shows the best fit of Eq. (2) assuming $r = 1.5$. The size effect law does not seem to fit perfectly through these points. This may be attributed to numerical scatter, which occurs due to mesh bias in coarse meshes, especially for smaller sizes. This is a natural consequence of the crack band model if the mesh size is fixed across all the sizes (that is, if no element size change with no post-peak slope adjustment is made). Dropping the smallest beam size would allow closer fits, but the conclusions would not change. A better fit is also possible if a refined mesh size—the same for all beam sizes—is introduced, but this would make simulating the larger sizes computationally prohibitive. Also note that here the authors impose $r = 1.5$ for simplicity, but in reality, the optimal value could be slightly different.

The resulting size effect law parameters for the three cases are: 1) plain concrete: $v_{u\infty}$ = 2.19 MPa (317.55 psi) and D_b = 157 mm (6.18 in.); 2) longitudinally reinforced concrete without stirrups: $v_{u\infty}$ = 2.21 MPa (320.45 psi) and D_b = 182 mm (7.165 in.); and 3) ditto with stirrups: $v_{u\infty}$ = 4.25 MPa (616.25 psi) and D_b = 158 mm (6.22 in.). It is seen that the trend of these values agrees with those from Data Set I. This confirms that, in all torsional strength of plain and reinforced concrete, a size effect of Type I is to be expected.

SUMMARY AND CONCLUSIONS

Based on the findings of this study, the following conclusions can be made:

1. The torsional strength of concrete structures exhibits a strong structural size effect. The size effect is exhibited not only by plain concrete beams and longitudinally reinforced concrete beams without stirrups, but also by longitudinally reinforced beams with stirrups. In all cases, the size effect is of Type I, which is the size effect for failures occurring at the moment of macrocrack initiation from the surface.

2. Consistent with experiments, the simulations show the torsional failure in plain concrete beams to be highly brittle, characterized by a sudden dynamic drop in the torque as soon as the peak load is reached.

3. The longitudinal reinforcement makes the failure less brittle, mitigating the sharp drop at peak. However, the peak torsional capacity is not increased appreciably, and the failure still occurs right at crack initiation.

4. The stirrups are confirmed to give a significant enhancement of the torsional capacity as well as ductility, manifested by lack of a steep load drop after peak. However, the type of size effect is still not altered by stirrups.

5. The size effect in reinforced beams with stirrups has been verified by simulations with the most advanced damage constitutive model for concrete, the microplane model M7. What enhances the credibility of these simulations is the fact that they fit the test data on other effects such as the reinforcement ratio and aspect ratio.

6. Future work should include torsional tests of beams with stirrups, especially with box cross sections, scaled up to large sizes.

FUTURE RESEARCH

It is, of course, desirable to confirm the present numerical findings by properly scaled torsion tests of reinforced concrete beams both with and without stirrups. An extension to combined torsion and bending is also needed.

AUTHOR BIOS

Kedar Kirane *is a Postdoctoral Fellow in the Department of Civil and Environmental Engineering at Northwestern University, Evanston, IL. He received his BE from University of Pune, Pune, India; his MS from Ohio State University, Columbus, OH; and his PhD from Northwestern University. His research interests include computational solid mechanics with an emphasis on fatigue and fracture of quasi-brittle materials.*

Konjengbam Darunkumar Singh *is an Associate Professor in the Department of Civil Engineering at the Indian Institute of Technology Guwahati, Guwahati, India. During research of this paper, he was a Visiting Scholar at Northwestern University, supported by Indo-US Research Fellowship.*

ACI Honorary Member **Zdeněk P. Bažant** *is McCormick Institute Professor and W.P. Murphy Professor of Civil and Mechanical Engineering and Materials Science at Northwestern University. He is a member and past Chair of Joint ACI-ASCE Committee 446, Fracture Mechanics of Concrete, and a member of ACI Committees 209, Creep and Shrinkage of Concrete, and 348, Structural Reliability and Safety; and Joint ACI-ASCE Committees 334, Concrete Shell Design and Construction; 445, Shear and Torsion; and 447, Finite Element Analysis of Reinforced Concrete Structures.*

ACKNOWLEDGMENTS

The authors wish to thank the U.S. National Science Foundation for partially supporting this research under Grant CMMI-1129449 to Northwestern University.

REFERENCES

1. Joint ACI-ASCE Committee 445, "Report on Torsion in Structural Concrete (ACI 445.1R-12)," American Concrete Institute, Farmington Hills, MI, 2013, 92 pp.

2. Hsu, T. T. C., "Torsion of Structural Concrete—Plain Concrete Rectangular Sections," *Torsion of Structural Concrete*, SP-18, American Concrete Institute, Farmington Hills, MI, Jan. 1968, pp. 203-238.

3. Hsu, T. T. C., "Torsion of Structural Concrete—Behavior of Reinforced Concrete Rectangular Members," *Torsion of Structural Concrete*, SP-18, American Concrete Institute, Farmington Hills, MI, Jan. 1968, pp. 261-306.

4. Bažant, Z. P., and Sener, S., "Size Effect in Torsional Failure of Concrete Beams," *Journal of Structural Engineering*, ASCE, V. 113, No. 10, 1987, pp. 2125-2136. doi: 10.1061/(ASCE)0733-9445(1987)113:10(2125)

5. Bažant, Z. P.; Sener, S.; and Prat, P. C., "Size Effect Tests of Torsional Failure of Plain and Reinforced Concrete Beams," *Materials and Structures*, V. 21, No. 6, 1988, pp. 425-430. doi: 10.1007/BF02472322

6. Hsu, T. T. C., and Mo, Y. L., "Softening of Concrete in Torsional Members—Theory and Tests," *ACI Journal Proceedings*, V. 82, No. 3, May-June 1985, pp. 290-303.

7. Humphreys, R., "Torsional Properties of Prestressed Concrete," *The Structural Engineer*, V. 35, No. 6, 1957, pp. 213-224.

8. Iravani, S., "Mechanical Properties of High-Performance Concrete," *ACI Materials Journal*, V. 93, No. 5, Sept.-Oct. 1996, pp. 416-426.

9. McMullen, A. E., and Daniel, H. R., "Torsional Strength of Longitudinally Reinforced Concrete Beams Containing an Opening," *ACI Journal Proceedings*, V. 72, No. 8, Aug. 1975, pp. 415-420.

10. McMullen, A. E., and Woodhead, H. R., "Experimental Study of Prestressed Concrete under Combined Torsion, Bending, and Shear," *PCI Journal*, V. 18, No. 5, 1973, pp. 85-100. doi: 10.15554/pcij.09011973.85.100

11. Rahal, K. N., "Torsional Strength of Reinforced Concrete Beams," *Canadian Journal of Civil Engineering*, V. 27, No. 3, 2000, pp. 445-453. doi: 10.1139/l99-083

12. Wang, W., and Hsu, T. T. C., "Limit Analysis of Reinforced Concrete Beams Subjected to Pure Torsion," *Journal of Structural Engineering*, ASCE, V. 123, No. 1, 1997, pp. 86-94. doi: 10.1061/(ASCE)0733-9445(1997)123:1(86)

13. Zia, P., "Torsional Strength of Prestressed Concrete Members," *ACI Journal Proceedings*, V. 57, No. 10, Oct. 1961, pp. 1337-1359.

14. Bažant, Z. P., and Planas, J., 1998, *Fracture and Size Effect in Concrete and Other Quasibrittle Materials*, CRC Press, Boca Raton, FL, 640 pp.

15. Caner, F. C., and Bažant, Z. P., "Microplane Model M7 for Plain Concrete I: Formulation," *Journal of Engineering Mechanics*, ASCE, V. 139, No. 12, 2013, pp. 1714-1723. doi: 10.1061/(ASCE)EM.1943-7889.0000570

16. Bažant, Z. P.; Caner, F. C.; Carol, I.; Adley, M. D.; and Akers, S. A., "Microplane Model M4 for Concrete: I. Formulation with Work-Conjugate Deviatoric Stress," *Journal of Engineering Mechanics*, ASEC, V. 126, No. 9, 2000, pp. 944-953. doi: 10.1061/(ASCE)0733-9399(2000)126:9(944)

17. Bažant, Z. P., and Oh, B. H., "Microplane Model for Progressive Fracture of Concrete and Rock," *Journal of Engineering Mechanics*, ASCE, V. 111, No. 4, 1985, pp. 559-582. doi: 10.1061/(ASCE)0733-9399(1985)111:4(559)

18. Caner, F. C., and Bažant, Z. P., "Microplane Model M7 for Plain Concrete II: Calibration and Verification," *Journal of Engineering Mechanics*, ASCE, V. 139, No. 12, 2013, pp. 1724-1735. doi: 10.1061/(ASCE)EM.1943-7889.0000571

19. Taylor, G. I., "Plastic Strain in Metals," *Journal of the Institute of Metals*, V. 62, 1938, pp. 307-324.

20. Batdorf, S., and Budianski, B., "A Mathematical Theory of Plasticity Based on the Concept of Slip," *Technical Note 1871*, National Advisory Committee for Aeronautics, Washington, DC, 1949.

21. Abaqus, *ABAQUS/Explicit User's Manual*, Abaqus Version 6.11, 2011.

22. Bažant, Z. P., and Oh, B. H., "Crack Band Theory for Fracture of Concrete," *Matériaux et Constructions*, V. 16, No. 3, 1983, pp. 155-177. doi: 10.1007/BF02486267

23. Bažant, Z. P., and Novák, D., "Energetic-Statistical Size Effect in Quasibrittle Failure at Crack Initiation," *ACI Materials Journal*, V. 97, No. 3, May-June 2000, pp. 381-392.

24. Bažant, Z. P., and Novák, D., "Probabilistic Nonlocal Theory for Quasibrittle Fracture Initiation and Size Effect. I. Theory," *Journal of Engineering Mechanics*, ASCE, V. 126, No. 2, 2000, pp. 166-174. doi: 10.1061/(ASCE)0733-9399(2000)126:2(166)